Chemical Rescue of a Site-Specific Mutant of Bacterial Copper Amine Oxidase for Generation of the Topa Quinone Cofactor†

Hideyuki Matsunami,‡,§ Toshihide Okajima,*,‡ Shun Hirota,|| Hiroshi Yamaguchi,⊥ Hiroshi Hori,# Minae Mure,‡ Shun'ichi Kuroda,‡ and Katsuyuki Tanizawa*,‡

Department of Structural Molecular Biology, Institute of Scientific and Industrial Research, Osaka University, Ibaraki, Osaka 567-0047, Japan, Department of Physical Chemistry, Kyoto Pharmaceutical University, Kyoto, Kyoto 607-8414, Japan, School of Science and Technology, Kwansei Gakuin University, Sanda, Hyogo 669-1337, Japan, and Graduate School of Engineering Science, Osaka University, Toyonaka, Osaka 560-8531, Japan

Received December 6, 2003; Revised Manuscript Received December 25, 2003

ABSTRACT: The topa quinone (TPQ) cofactor of copper amine oxidase is produced by posttranslational modification of a specific tyrosine residue through the copper-dependent, self-catalytic process. We have site-specifically mutated three histidine residues (His431, His433, and His592) involved in binding of the copper ion in the recombinant phenylethylamine oxidase from *Arthrobacter globiformis*. The mutant enzymes, in which each histidine was replaced by alanine, were purified in the Cu/TPQ-free precursor form and analyzed for their Cu-binding and TPQ-generating activities by UV−visible absorption, resonance Raman, and electron paramagnetic resonance spectroscopies. Among the three histidine-to-alanine mutants, only H592A was found to show a weak activity to form TPQ upon aerobic incubation with Cu^{2+} ions. Also for H592A, exogenous imidazole rescued binding of copper and markedly promoted the TPQ formation. Accommodation of a free imidazole molecule within the cavity created in the active site of H592A was suggested by X-ray crystallography. Although the TPQ cofactor in H592A mutant was readily reduced with substrate, its catalytic activity was very low even in the presence of imidazole. Combined with the crystal structures of the mutant enzymes, these results demonstrate the importance of the three copper-binding histidine residues for both TPQ biogenesis and catalytic activity, fine-tuning the position of the essential metal.

Copper amine oxidases (EC 1.4.3.6) require a redox-active organic cofactor, topa quinone (TPQ[1]), to catalyze the oxidation of various primary amine substrates (*1*−*3*). In all genes coding for the enzymes from both prokaryotic and eukaryotic organisms (*4*−*6*), the TPQ cofactor is invariantly encoded by a tyrosine codon and produced by posttranslational oxidative modification of the tyrosine residue that proceeds in a copper-dependent, self-processing reaction (*7*−*10*). X-ray crystallographic structures of the enzymes belonging to this family have so far been determined for the enzymes with distinct substrate specificities; tyramine oxidase from *Escherichia coli* (ECAO) (*11, 12*), diamine oxidase from pea seedling (PSAO) (*13*), phenylethylamine oxidase from *Arthrobacter globiformis* (AGAO) (*14*), and methylamine oxidase from *Hansenula polymorpha* (HPAO) (*15*). These structural studies have revealed their very high similarities in the overall polypeptide fold, active-site structure, and coordination geometry characteristic of the nonblue, type-II Cu atom, which is coordinated with three invariant histidine residues and two water molecules in a distorted square-pyramidal geometry.

For AGAO, the structures of both the inactive precursor form containing an unmodified tyrosine residue (designated apo-AGAO) and the active mature form containing a Cu atom and TPQ (holo-AGAO) have been solved (*14*). The two structures were found to be almost superimposable, suggesting that the structural changes during the Cu-dependent TPQ formation are limited to the active site. An important finding obtained from the structural comparison is that the imidazole ring of one of the three Cu-binding histidine residues, His592, can adopt two distinct conformations (conformers *a* and *b*) in the two crystal structures, whereas those of the other two histidine residues, His431 and His433, are restricted only in a single conformation. The presumed flexibility of His592 appeared to be important for changes in the coordination structure of the Cu atom, which would play a crucial role in activating the precursor tyrosine ring for

† This study was supported by Grants-in-Aid for Scientific Research from the Ministry of Education, Culture, Sports, Science and Technology of Japan (Priority Areas, No. 13125204; the 21st Century Center of Excellence Program, K.T.) and from the Japan Society for the Promotion of Science (Category B, No. 12480180, K.T.; Category C, No. 14560066, T.O.).

* To whom correspondence should be addressed. Tel.: +81-6-6879-8461. Fax: +81-6-6879-8464. E-mail: tokajima@sanken.osaka-u.ac.jp or tanizawa@sanken.osaka-u.ac.jp.

‡ Institute of Scientific and Industrial Research, Osaka University.

§ Current address: Namba Protonic NanoMachine Project, ERATO, JST, 3-4 Hikaridai, Seika, Souraku, Kyoto 691-0237, Japan.

|| Kyoto Pharmaceutical University.

⊥ Kwansei Gakuin University.

Graduate School of Engineering Science, Osaka University.

[1] Abbreviations: TPQ, topa quinone; AGAO, phenylethylamine oxidase from *Arthrobacter globiformis*; ECAO, tyramine oxidase from *Escherichia coli*; PSAO, diamine oxidase from pea seedling; HPAO, methylamine oxidase from *Hansenula polymorpha*; EPR, electron paramagnetic resonance; RR, resonance Raman; Hepes, 4-(2-hydroxyethyl)-1-piperazineethanesulfonic acid; PCR, polymerase chain reaction; WT, wild type; SDS−PAGE, sodium dodecyl sulfate−polyacrylamide gel electrophoresis; LMCT, ligand-to-metal charge transfer.

10.1021/bi0361923 CCC: $27.50
Published on Web 02/05/2004

the attack by dioxygen and in properly coordinating water molecules during the TPQ biogenesis (*14*). More recently, we have analyzed the process of TPQ biogenesis by time-resolved X-ray crystallography and determined the structures of freeze-trapped intermediates (*16*). During the process, the imidazole side chains of His431 and His433 maintain a single conformation that is almost identical with those in the apo- and holo-AGAO structures, while that of His592 exists in two conformations with different proportions in each intermediate, supporting the conformational flexibility of His592.

To elucidate the molecular mechanism of TPQ biogenesis in copper amine oxidase and the role(s) of the Cu-binding histidine residues, we have replaced each histidine residue of AGAO with an alanine residue by site-specific mutagenesis. The mutant enzymes have been purified in the Cu/TPQ-free precursor form and analyzed for their abilities to bind a Cu^{2+} ion and to generate the TPQ cofactor by UV−visible absorption, electron paramagnetic resonance (EPR), and resonance Raman (RR) spectroscopies, as well as by X-ray crystallography. Here we show that the His592-to-Ala mutant can be chemically rescued by exogenous imidazole in binding of a Cu^{2+} ion and self-processed formation of TPQ. In accord with the dual conformations of His592 observed by X-ray crystallography (*14*), the mutation of His592 to alanine is assumed to have created enough of a cavity in the Cu-binding site to accommodate a free imidazole molecule, which assists Cu-binding. The results presented in this paper highlight the importance of the copper coordination structure afforded by the three histidine residues for both TPQ biogenesis and catalytic activity.

EXPERIMENTAL PROCEDURES

Materials. 4-(2-Hydroxyethyl)-1-piperazineethanesulfonic acid (Hepes) was purchased from Dojindo Lab., Co. (Kumamoto, Japan); imidazole, $CuSO_4 \cdot 5H_2O$, and phenylhydrazine·HCl were from Nacalai Tesque (Kyoto, Japan); and 2-phenylethylamine·HCl was from Wako Pure Chemicals (Osaka, Japan). Isotopically enriched ^{63}Cu was obtained as a metal wire (0.5 g, 99.1 at. %) from ICON (Summit, NJ), dissolved in 2 N nitric acid, and crystallized as $CuCl_2 \cdot 2H_2O$.

Site-Specific Mutagenesis. Site-specific mutagenesis for His431, His433, and His592, each to be replaced by alanine (designated H431A, H433A, and H592A, respectively), was performed by the two-step polymerase chain reaction (PCR) essentially according to the method of Ho et al. (*17*) using the following pairs of mutually complementary primers (+, sense strand; −, antisense strand) containing mismatching bases (italic) for the mutated codons: H431A (+), 5′-AGCGCCGTTC*GCC*CAGCACAT-3′; H431A (−), 3′-CCTCGCGGCAAG*CGG*GTCGTGTAGAAG-5′; H433A (+), 5′-TTCCACCAG*GCC*ATCTTCAGCG-3′; H433A (−), 3′-GGCAAGGTGGTC*CGG*TAGAAGTCGCGG-5′; H592A (+), 5′-CTTCGGACTGACC*GCC*TTCCCGCGC-3′; H592A (−), 3′-AAGCCTGACTGG*CGG*AAGGGCGCGCACC-5′; primer I (+), 5′-GCTCCGGCCCATCATCAA-3′; primer II (−), 3′-CGACAGGCGCTCCGGCTAC-5′; primer III (+), 5′-CAACAGGTGGAGGAAGA-3′; primer IV (−), 3′-GGTGGCGACTCGTTATTGATC-5′.

Primers I and II, which were used for constructing H431A and H433A mutants as the common forward (+) and reverse (−) primers in each PCR, corresponded to nucleotides 801−818 and 1447−1465, respectively, of the AGAO gene with the first A of the initiator ATG codon numbered as nucleotide 1 (*18*). Similarly, primers III and IV, which were used for constructing H592A mutant, corresponded to nucleotides 1341−1358 and 1971−1991, respectively. In the first PCR with plasmid pPEAO2 encoding wild-type (WT) enzyme (*18*) as a template, two separate reactions were carried out using each pair of two primers [primer I or III plus one of the reverse (−) mutagenic primers, and primer II or IV plus the other counterpart of the forward (+) mutagenic primers]. The two PCR products were filtered through Suprec-02 cartridges (Takara Shuzo) to remove excess primers, annealed with each other (94 °C for 10 min, 40 °C for 10 min), and extended at 72 °C for 3 min by Taq DNA polymerase. The second PCR was done with the double-stranded fragment obtained above as a template and primers I and II (for H431A and H433A) or primers III and IV (for H592A). A 555-bp *Spl* I−*Mul* I or 541-bp *Mul* I−*Xho* I fragment excised from the amplified DNA was substituted for the corresponding fragment in pPEAO2. The sequence of the inserted region was confirmed with an Applied Biosystems 370A DNA sequencer. The resulting constructs were used to transform *E. coli* BL21 (DE3) cells for expression of the mutant proteins.

Enzyme Purification and Activation by Cu^{2+} Ion. The WT and mutant enzymes of AGAO were overproduced in *E. coli* BL21 (DE3) cells grown on an M9 medium supplemented with 0.4% tryptone (Difco Lab., Detroit, MI), 0.4% glucose, and 50 μg/mL ampicillin. The enzymes were purified to homogeneity as the Cu/TPQ-free precursor protein (apo form) according to the method reported previously (*7*). The levels of protein expression and the yields of purified protein for the three histidine-to-alanine mutants were similar to the WT AGAO. Purity of the WT and mutant enzymes was checked by sodium dodecyl sulfate−polyacrylamide gel electrophoresis (SDS−PAGE). Protein concentrations were determined using extinction coefficients at 280 nm of 12.3 and 13.2 for 10 mg/mL solutions of apo- and holo-AGAO, respectively (*7*), and calculated as subunit concentration with an approximate M_r of 70 600 (*18*). Conversion of apo-WT and -mutant enzymes into holo forms was generally performed by incubating each apo enzyme (0.1 mM subunit) with 0.5 mM $CuSO_4$ in 25 mM Hepes (pH 6.8) at 25 °C for 24 h. Unbound and weakly bound Cu^{2+} ions were removed by dialysis against 25 mM Hepes (pH 6.8) containing 4 mM EDTA for 12 h, followed by thorough dialysis against 25 mM Hepes (pH 6.8) alone for 12 h. These copper-loaded samples of WT and mutant enzymes were used for the solution studies in the presence or absence of imidazole (10 mM, unless otherwise stated).

Enzyme Assay and Measurements of Cu and TPQ Contents. The catalytic activity with 2-phenylethylamine as substrate was assayed by monitoring H_2O_2 production coupled to the oxidation of 2,2′-azinobis(3-ethylbenzthiazoline-6-sulfonic acid) ($\epsilon_{414nm} = 24\,600\ M^{-1}\ cm^{-1}$) by horseradish peroxidase (Wako Pure Chemicals, Osaka, Japan) as described previously (*7*). The method of titration of TPQ with phenylhydrazine was identical with that reported previously (*7*); the phenylhydrazine solution used was freshly prepared by dissolving the reagent recrystallized from methanol. The Cu contents in the enzyme proteins were analyzed at 324.8 nm with a Shimadzu AA-6400G atomic

absorption spectrophotometer attached with a GFA-4A graphite furnace atomizer, using an atomic-absorption-analysis-grade $CuSO_4$ solution in 0.1 M HNO_3 as the internal and external standards.

Spectroscopic Measurements. UV−visible absorption spectra were measured with a Hewlett-Packard 8452A photodiode-array spectrophotometer. For anaerobic reduction with substrate, WT and H592A mutant (0.1 mM subunit in 25 mM Hepes, pH 6.8) were evacuated in an anaerobic chamber and flushed with argon gas to remove dissolved oxygen. 2-Phenylethylamine (final concentration, 0.4 mM) was anaerobically added with a gastight syringe to each enzyme solution prepared in a tightly sealed quartz cell with a 1-cm light path, and the absorption spectra were measured immediately. EPR spectra were measured on a home-built EPR spectrometer by using a Varian X-band cavity equipped with an Oxford Instruments cryostat (ESR-900). Recording conditions were as follows: temperature, 77 K; microwave power, 5 mW; frequency, 9.36 GHz; modulation amplitude, 5 G; scan time, 2 s; repetition, 4 times; time constant, 10 ms. The magnetic field strength was determined by nuclear magnetic resonance of protons in water. RR scattering was excited at 514.5 nm with an Ar^+ ion laser (Spectra Physics, 2017) and detected with a triple polychromator (JASCO, NR-1800) equipped with a CCD detector (Princeton Instruments). The slit width and height were set to 100 μm and 15 μm, respectively. The excitation laser beam power was adjusted to 70 mW at the sample point. RR spectra were measured at ambient temperature in a spinning cell (3000 rpm). The data accumulation time was 200 s. Raman shifts were calibrated with acetone and toluene, and the accuracy of the peak positions of the Raman bands was ± 1 cm^{-1}.

X-ray Crystallographic Analysis. The purified mutant enzymes were crystallized at 16 °C by the microdialysis method (*14*, *19*). Before crystallization, H592A mutant was first incubated with 0.5 mM $CuSO_4$ and 5 mM imidazole at 4 °C for 24 h to fully reconstitute with Cu^{2+} ions. The protein concentration in the dialysis button (volume, 50 μL) was 10 mg/mL, and the reservoir solution contained 1.05 M potassium sodium tartrate as a precipitant in 25 mM Hepes, pH 6.8. Rod-shaped crystals (approximate size, 0.8 mm × 0.2 mm × 0.2 mm) obtained after about 2 weeks were equilibrated in a solution containing 45% glycerol (cryoprotectant), 0.2 M potassium sodium tartrate, and 25 mM Hepes (pH 6.8) for 3 days. As for H433A mutant, the enzyme was first crystallized in the apo form and soaked with the buffer containing 2 mM $CuSO_4$ at about 15 min before the data collection. The crystals were mounted on thin nylon loops (ϕ, 0.2−0.3 mm) and frozen by flash cooling to 100 K in a cold N_2 gas stream. Diffraction data sets were collected at 100 K with the synchrotron X-radiation (λ = 1.0 and 0.85 Å) using an imaging plate and an ADSC CCD detector for H433A and H592A, respectively, in the station BL44B2 at the SPring-8 (Hyogo, Japan). The data were processed and scaled using DENZO/SCALEPACK (*20*) for H433A or MOSFLM (*21*) and SCALA (*22*) for H592A. These crystals were found to belong to a space group of *I*2, as reported for the WT crystals solved at 100 K (*19*). An initial model for the AGAO dimer was generated by 180° rotation around the crystallographic 2-fold axis of the monomer coordinates (PDB accession code 1AVK) without solvent molecules. The program used for refinements and calculation of the electron-density maps was X-PLOR, version 3.851 (*23*). Manual rebuilding and assignment of solvent molecules were performed using QUANTA, version 97 (Accelrys, San Diego, CA). After rigid-body refinement, initial structures of H433A and H592A were further refined through simulated annealing at 3000 K and several cycles of positional and B-factor refinements. Metal ions were assigned on the basis of the highest peaks in the respective $2F_o - F_c$ maps; water molecules and residues in the active site region for the two mutant enzymes were carefully modeled using the $2F_o - F_c$, $F_o - F_c$, and omit maps. The details and statistics of crystallographic refinement for the mutant structures are summarized in Table 1.

Table 1: Statistics of Data Collection and Refinement

protein	H433A-AGAO	H592A-AGAO
Data Collection		
cell		
space group	*I*2	*I*2
unit cell dimension *a*, *b*, *c* (Å), β (deg)	156.51, 63.32, 185.21,111.50	157.76, 63.21, 184.24, 111.64
no. of obsns	277 010	912 205
no. of unique reflns	107 167	220 460
$d_{max} - d_{min}$ (Å)	100−2.0	23.8−1.6
overall completeness (%)	93.9	99.3
overall R_{merge} (%)[a]	8.4	6.7
Refinement Statistics		
$d_{max} - d_{min}$ (Å)	10−2.0	10−1.8
residues in the core ϕ,φ regions (%)	85.6	88.9
no. of non-hydrogen atoms	10485	10839
no. of solvent atoms	759	1107
average temperature factor		
main-chain (Å^2)	23.6	15.4
side-chain atoms (Å^2)	24.2	17.1
solvent atoms (Å^2)	31.8	27.7
rms deviation from ideal values		
bond lengths (Å)	0.009	0.008
bond angles (deg)	1.6	1.5
residual *R* (%) [b]	20.7	21.9
free residual *R* (%)[c]	28.0	25.9

[a] $R_{merge} = \sum h \sum i |I_{h,i} - \langle I_h \rangle| / \sum h \sum i I_{h,i}$, where $I_{h,i}$ is the intensity value of the *i*th measurement of *h*, and $\langle I_h \rangle$ is the corresponding mean value of I_h for all *i* measurements. [b] $R = \sum ||F_o| - |F_c|| / \sum |F_o|$. [c] Free residual *R* is an *R* factor of the X-PLOR refinement evaluated for 5% of the reflections that were excluded from the refinement.

The atomic coordinates and structure factors for the H433A and H592A mutant enzymes have been deposited in the Protein Data Bank with the accession codes 1UI7 and 1UI8, respectively.

RESULTS

Mutation of Copper-Binding Histidine Residues. The three histidine residues (His431, His433, and His592) involved in binding of the Cu atom in AGAO have been substituted individually with alanine by PCR-based site-specific mutagenesis. The H431A, H433A, and H592A mutant enzymes purified to homogeneity in the apo forms showed UV−visible absorption spectra identical with that of apo-WT enzyme, in which the 485-nm absorption peak characteristic of the oxidized form of the TPQ cofactor in holo-AGAO (*7*) was absent. By incubation with excess Cu^{2+} ions under aerobic conditions, WT enzyme is readily activated as a result

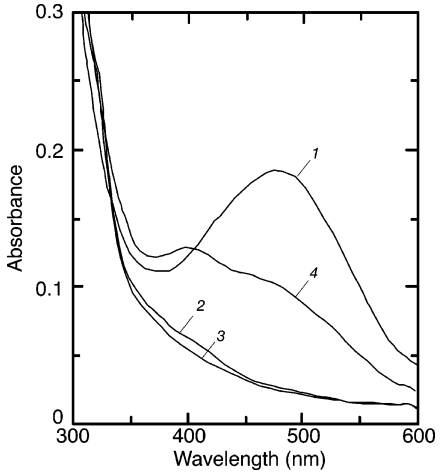

FIGURE 1: Absorption spectra of Cu-reconstituted WT and histidine mutant enzymes of AGAO. The purified apo forms of WT and mutant enzymes (0.1 mM subunit) were incubated with 0.5 mM Cu^{2+} at 25 °C for 24 h and dialyzed against 25 mM Hepes, pH 6.8, for 24 h: curve 1, WT; curve 2, H431A; curve 3, H433A; curve 4, H592A.

Table 2: Characteristics of Cu^{2+}/Imidazole (Imd)-Reconstituted WT and Histidine Mutant Enzymes

	Cu content[a] (mol atom/subunit)		specific activity (units/mg)		TPQ content[b] (mol/subunit)	
enzyme	− Imd	+ Imd[c]	− Imd	+ Imd[c]	− Imd	+ Imd[c]
WT	0.93	0.94	59	58	0.82	0.79
H431A	0.08	0.27	0	0	0	0
H433A	0.41	0.42	0.001	0.002	0.01	0.01
H592A	0.20	0.62	0.020	0.028	0.053	0.40

[a] Determined by atomic absorption. [b] Determined by titration with phenylhydrazine. [c] 10 mM.

of the formation of TPQ that proceeds by self-processing (*7*) (Figure 1, curve 1). However, no spectral change was observed with H431A and H433A mutants even after 24-h incubation with Cu^{2+} ions under the fully O_2-saturated conditions (curves 2 and 3). With H592A mutant, there was a small increase in the 350−600-nm region of the absorption spectrum (curve 4), suggesting that TPQ was formed only partially.

After incubation with excess Cu^{2+} ions for 24 h, WT and mutant enzymes were thoroughly dialyzed for removal of unbound or weakly bound Cu^{2+} ions. Their copper contents measured by atomic absorption analysis, specific activities assayed with 2-phenylethylamine as substrate, and TPQ contents determined by titration with phenylhydrazine (*7*) are summarized in Table 2. WT enzyme contained stoichiometric amounts of the Cu atom and the TPQ cofactor[2] and showed very high catalytic activity. In contrast, all the mutant enzymes had considerably decreased Cu contents and negligible catalytic activities with practically undetectable or very low TPQ contents. Therefore, any one of His431, His433, and His592 is very important for stable binding of the Cu atom and thereby essential for TPQ formation. It is noteworthy that the three histidine residues contribute differently in copper binding; in view of the Cu contents in

[2] In titration of TPQ with phenylhydrazine, a value less than 1.0 equiv of TPQ per subunit has been usually obtained for most copper amine oxidases (*2*), which may be due to the half-of-the-sites reactivity of TPQ in the dimeric enzyme with phenylhydrazine (*24*).

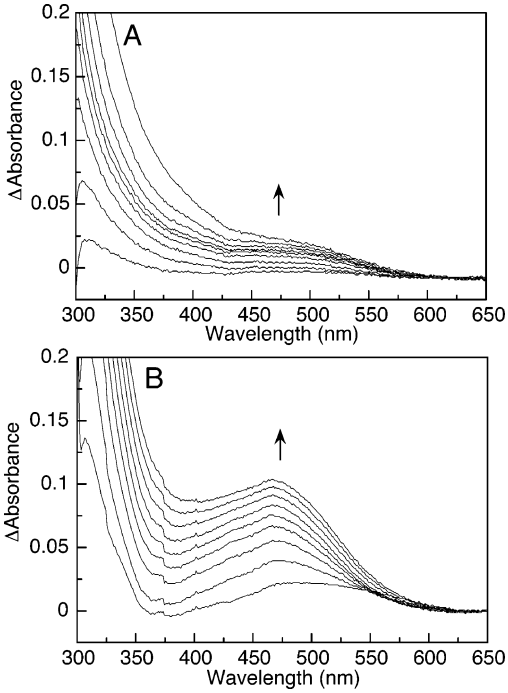

FIGURE 2: Spectral changes of H592A upon incubation with Cu^{2+} ion. H592A (0.1 mM subunit) was incubated with 0.5 mM Cu^{2+} in the absence (A) and presence (B) of 2.5 mM imidazole. Spectra were recorded at 1-h intervals and shown as difference spectra by subtracting the spectrum at 0 h (before incubation). Arrows indicate the direction of spectral change.

the mutant enzymes (Table 2), the importance of the imidazole side chain is in the decreasing order of His431, His592, and His433, although His592 is less important for TPQ formation than His431 and His433.

Chemical Rescue by Exogenous Imidazole. Addition of free imidazole to the TPQ biogenesis reaction mixture had almost no effect on WT, H431A, and H433A mutant enzymes (Table 2). However, exogenous imidazole significantly affected the Cu^{2+} ion-dependent TPQ formation in H592A mutant. Shown in Figure 2A,B are the spectral changes associated with the TPQ formation in H592A mutant in the absence and presence of imidazole, respectively. Observed pseudo-first-order rate constants for the increase of the absorption peak at 485 nm were about 0.15 h^{-1} (0.0025 min^{-1}) and 1.2 h^{-1} (0.02 min^{-1}) in the absence and presence of 10 mM imidazole, respectively. These rates are extremely slow when compared to that of TPQ biogenesis in the WT enzyme reported previously (k_{obs} = ∼1.5 min^{-1}) (*25*). Nevertheless, the chemical rescue by exogenous imidazole is evident with H592A mutant, giving a TPQ content increased by about 10 times that formed in its absence (Table 2). From the Cu contents determined after dialysis (Table 2), it appears that imidazole stabilizes the Cu-binding to H592A mutant (and, to a lesser extent, to H431A). Other imidazole derivatives including 1-methyl-, 2-methyl-, and 4-methylimidazoles were ineffective for TPQ formation in H592A mutant, showing that the chemical rescue is structurally limited only to the unsubstituted imidazole.

Identity of TPQ generated in H592A mutant in the presence of imidazole was confirmed by measuring the RR spectra, in which the spectrum of the Cu-free precursor protein was subtracted to obtain the RR spectrum of TPQ without protein-derived vibrational modes (*26, 27*). The RR

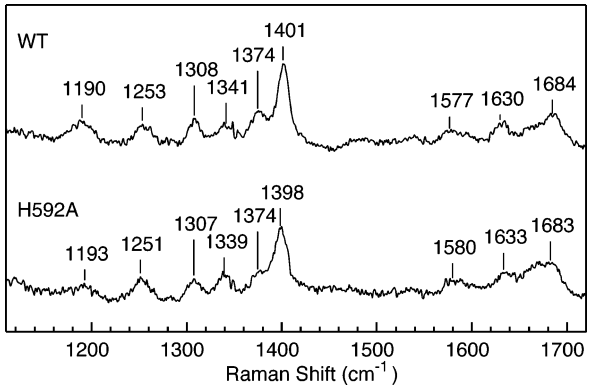

FIGURE 3: RR spectra of holo-WT and -H592A. RR spectra of WT (upper) and Cu^{2+}/imidazole-rescued H592A (lower) (1.0 mM subunit; for H592A, the apo enzyme was activated in the presence of 10 mM imidazole) were recorded at room temperature in 25 mM Hepes, pH 6.8. Frequency shifts calibrated with acetone and toluene standards (not shown) are indicated above the peaks. Instrumental conditions are described under Experimental Procedures.

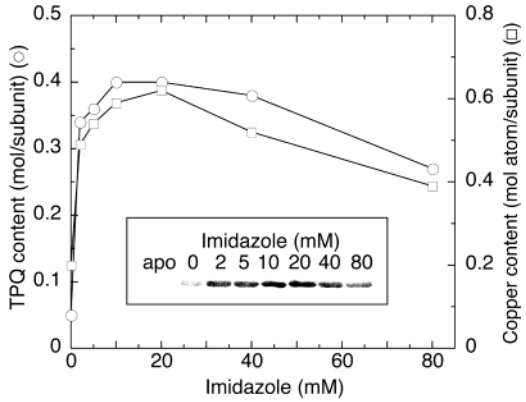

FIGURE 4: Effect of exogenous imidazole on TPQ formation in H592A. H592A (1.0 mM subunit) was incubated for 24 h with 2 mM Cu^{2+} in the presence of various concentrations (0−80 mM) of exogenous imidazole. Copper (○) and TPQ (□) contents of the resultant H592A protein were determined and plotted against imidazole concentration. In the inset, for quinone staining (*28*), 5 μg of the protein was applied to SDS−PAGE and the protein bands were electrotransferred onto a nitrocellulose membrane.

spectrum of H592A mutant clearly shows its Raman bands almost identical with those characteristic of TPQ in the WT enzyme (Figure 3), each wavenumber corresponding within ± 3 cm^{-1}.

The effect of imidazole concentration on the TPQ formation in H592A mutant was investigated by incubating with Cu^{2+} ions in the presence of 0−80 mM imidazole for 24 h, followed by thorough dialysis against 25 mM Hepes buffer, pH 6.8, containing 4 mM EDTA. The TPQ generated were determined by titration with phenylhydrazine and also visualized with the alkaline nitroblue tetrazolium/glycinate reagent developed for quinone staining (*28*). As shown in Figure 4, the TPQ content appeared to be saturated with respect to the imidazole concentration below 20 mM, which suggested reversible binding of imidazole. An apparent K_m value for imidazole was estimated to be about 1.7 mM. Higher concentrations (above 20 mM) of imidazole, however, were rather inhibitory for Cu-binding and TPQ formation, probably because of its chelating activity to Cu^{2+} ions.

^{63}Cu EPR Spectra. EPR spectra were measured at 77 K for the WT and mutant enzymes after reconstitution with a

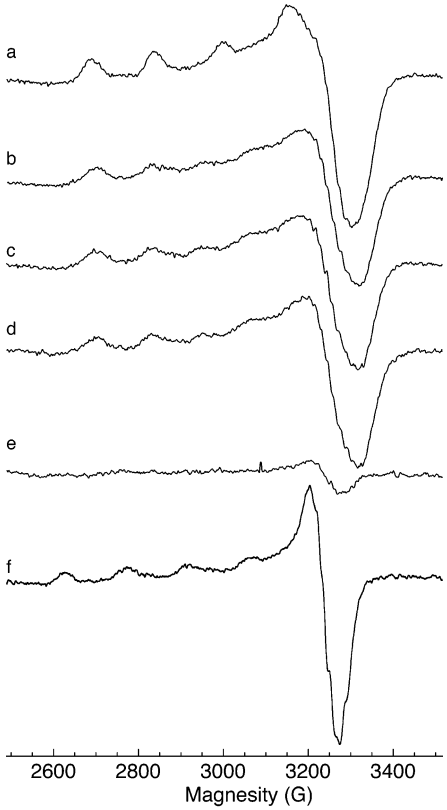

FIGURE 5: EPR spectra of ^{63}Cu-reconstituted WT and mutant enzymes. Spectra a−d were obtained with approximately the same volumes of the WT and mutant enzymes (0.5 mM subunit) mixed with 0.5 mM Cu^{2+}: (a) WT; (b) H431A; (c) H433A; (d) H592A. Apo-H592A (0.5 mM subunit) was incubated at 25 °C for 24 h with 1 mM Cu^{2+} in the absence (e) and presence (f) of 5 mM imidazole and dialyzed at 4 °C for 24 h against 25 mM Hepes, pH 6.8, containing 4 mM EDTA and then at 4 °C for 24 h against 25 mM Hepes, pH 6.8, alone. Instrumental conditions are described under Experimental Procedures.

stoichiometric amount of magnetically uniform ^{63}Cu(II). As reported for the holo-AGAO (*29*), the spectrum of the WT enzyme exhibited a typical feature of the type-II Cu center with spin Hamiltonian parameters of $g_{||} = 2.28$, $g_{\perp} = 2.05$, and $A_{||} = 15.9$ mT, indicating that most of the added Cu is bound to the enzyme protein (Figure 5, curve a). In contrast, the EPR spectra of the mutant enzymes were apparently a mixture of the type-II Cu and free Cu^{2+} ions (curves b−d). Furthermore, these EPR signals disappeared considerably upon extensive dialysis of the mutant enzymes (curve e). Thus, the Cu-binding is weaker in the mutant enzymes than in the WT enzyme, most likely due to the absence of one of the three Cu-binding histidine residues. Addition of free imidazole again led to stable binding of Cu only for H592A mutant, giving rise to the EPR signals with spin Hamiltonian parameters of $g_{||} = 2.34$, $g_{\perp} = 2.06$, and $A_{||} = 14.2$ mT (curve f). The differences in EPR spectra and parameters of WT and H592A enzymes suggest that the Cu-coordination geometry in the imidazole-rescued H592A mutant is slightly different (more rhombic) from that in the WT enzyme. This is consistent with the Cu-coordination structure observed in the crystal structures, as described later.

Reactivity with Amine Substrate. It is conceivable that the H431A and H433A mutant enzymes have almost no activity without TPQ cofactor (Table 2). However, the catalytic activity of H592A, in which TPQ has been formed signifi-

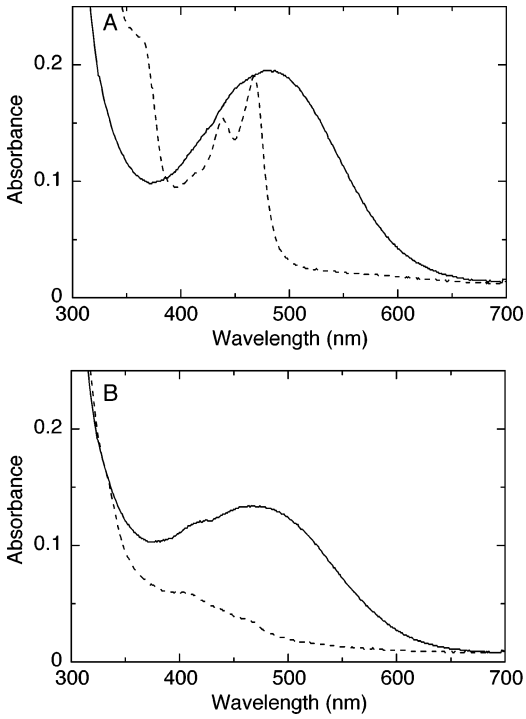

FIGURE 6: Spectral change upon reduction with substrate amine. Absorption spectra were measured for WT (A) and Cu^{2+}/imidazole-rescued H592A (B) (0.1 mM subunit; for H592A, the apo enzyme was activated in the presence of 10 mM imidazole) before (—) and after (− − −) incubation with 0.4 mM phenylethylamine in 25 mM Hepes, pH 6.8, under anaerobic conditions.

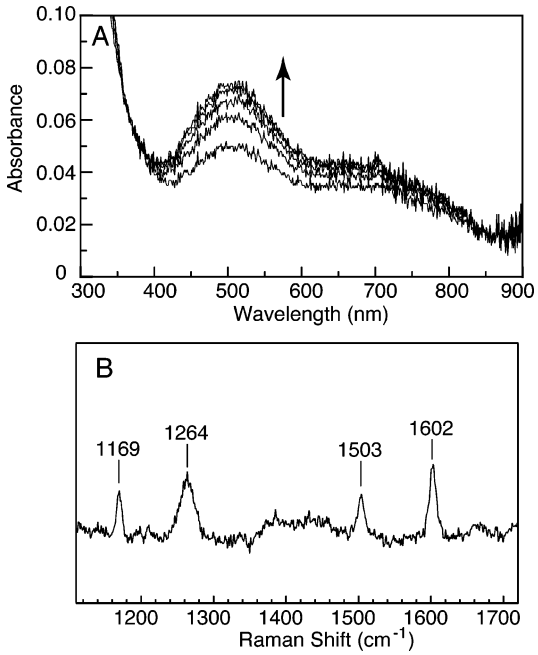

FIGURE 7: Absorption and RR spectra of H433A reconstituted with Cu^{2+} ion. Absorption spectra (A) were recorded at every 1 min after mixing H433A (0.1 mM subunit) with 0.2 mM Cu^{2+}. An arrow indicates the direction of spectral change. RR spectrum (B) was recorded immediately after mixing H433A (0.1 mM subunit) with 0.2 mM Cu^{2+}. Instrumental conditions are described under Experimental Procedures.

cantly by imidazole rescue, is also very low irrespective of the presence of imidazole (Table 2). Thus, the free imidazole has little effect on the catalytic activity of Cu/TPQ-containing H592A. However, the TPQ cofactor in H592A should be catalytically competent because it could be titrated with the inhibitor phenylhydrazine. Indeed, the absorption band at about 480 nm of the oxidized TPQ in H592A disappeared immediately upon addition of substrate, 2-phenylethylamine, under anaerobic conditions (Figure 6B), showing that TPQ was reduced to an aminoresorcinol form. This suggests that the catalytic reaction by H592A proceeds through the reductive half-reaction, comprising the former half of the overall ping-pong mechanism (*19*), and hence that the decreased activity of Cu/TPQ-containing H592A mutant is mainly ascribed to the latter oxidative half-reaction. Using the metal-substituted AGAO, we have reported that the bound Cu participates in the oxidative half-reaction by providing a binding site for $1e^-$- and $2e^-$-reduced dioxygen species to be efficiently protonated and released (*19*). Therefore, it is assumed that the Cu-coordination structure of H592A with a free imidazole as one of the Cu-ligands is ineffective for catalysis, particularly in the oxidative half-reaction. Furthermore, it is noteworthy that in H592A the semiquinone radical of TPQ is little formed from the reduced TPQ, unlike the WT enzyme (Figure 6A), in which $1e^-$-transfer occurs from the reduced TPQ to the bound Cu under anaerobic conditions (*19*, *30*). The absence of a semiquinone state in the imidazole-rescued H592A following substrate reduction may be another possible reason for its negligible catalytic activity.

Formation of a Charge-Transfer Complex in H433A. Although the TPQ cofactor was not formed in the H433A mutant by incubation with Cu^{2+} ions (Table 2), we noted that the solution slightly colored red soon after addition of Cu^{2+} ions to the purified apo-H433A. We therefore monitored the spectral changes that occurred within several minutes after addition of Cu^{2+} ions to H433A (Figure 7A). The observed spectrum was dissimilar to that of TPQ, having an absorption peak at about 500 nm and a shoulder band extending to a longer wavelength region of 600−800 nm. Although the color faded away gradually on further incubation (>30 min), it was considerably stable under anaerobic conditions. Upon irradiation of laser light at 514.5 nm at about 5 min after addition of Cu^{2+} ions, enhancement of RR scattering was observed for the bands at 1169, 1264, 1503, and 1602 cm^{-1}, as shown in Figure 7B. The RR spectrum is much simpler than that of TPQ (cf. Figure 3). These absorption and RR features closely resemble those of a ligand-to-metal charge-transfer (LMCT) complex reported for galactose oxidase (*31*, *32*) and for model compounds (*33*). However, on the basis of the molar extinction coefficient of the tyrosinate-to-copper charge-transfer complex in galactose oxidase (ϵ = 9500 M^{-1} cm^{-1} at 445 nm) (*34*), the LMCT complex formed in the H433A mutant of AGAO is estimated from the absorbance at 500 nm to account for only 8% of the total enzyme species.

Crystal Structures of H433A and H592A Mutants. The crystal structures of the H433A mutant soaked with Cu^{2+} ion and the imidazole-rescued holo-H592A mutant have been determined at 100 K. The overall structures of H433A and H592A mutants were essentially identical with the WT-AGAO structure solved at 100 K (*16*), giving root-mean-square deviations of 0.50 and 0.37 Å, respectively, for the coordinates of all main chain atoms. The Cu^{2+} ion was also found to occupy almost the same position as in the WT

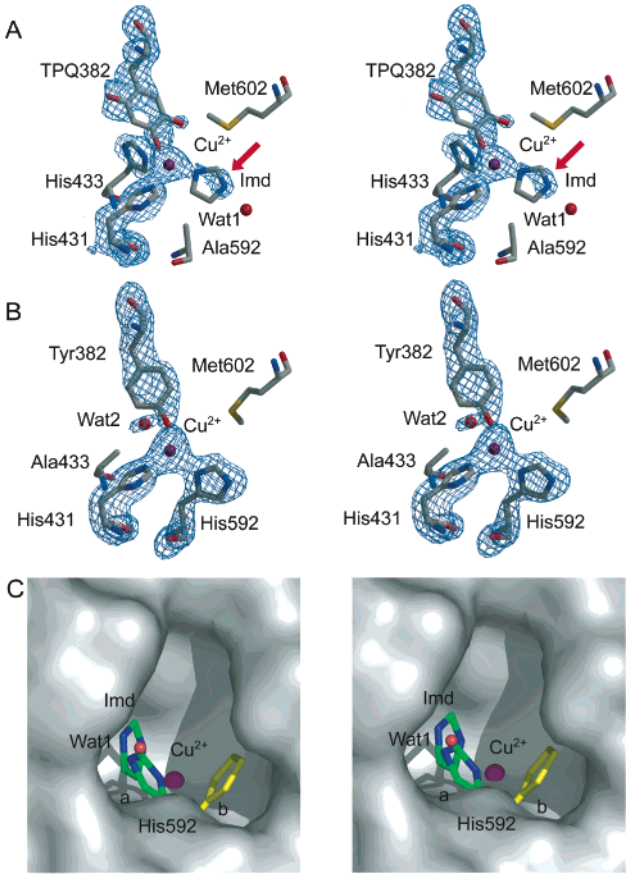

FIGURE 8: Stereoviews of active site structures. The annealed $F_o - F_c$ omit maps (A, H592A; B, H433A) for the region within 3 Å from the copper center are contoured at 3.0σ and shown with the final model. A modeled exogenous imidazole (Imd) is also shown in panel A. Panel C shows a stereodiagram of molecular surface of the cavity produced in H592A mutant, viewed from the intersubunit space and drawn with an accommodated imidazole (Imd) and Wat1. Major (*a*) and minor (*b*) conformers of His592 in WT (PDB code 1AV4), colored green and yellow, respectively, are also shown in stick model. Figures were generated with Bobscript (*42*) and Raster 3D (*43*) for panels A and B and with a PyMol molecular graphic system (DeLano Scientific, San Carlos, CA) for panel C.

enzyme. Significant differences were noted only for the active-site residues and crystallographically identified water molecules.

In the active site of H592A, the TPQ ring is modeled to point directly toward the bound Cu atom (Figure 8A), taking a "Cu-on" conformation previously observed in the WT-AGAO structure determined at an ambient temperature (*14*). Thus, the Cu atom is four-coordinate with the $N^{\epsilon 2}$ atoms of His431 and His433 and the O4 and O5 atoms of TPQ382. Within the space created by the mutation of His592 to alanine, there is an extra electron density in the $F_o - F_c$ omit map contoured at 3.0σ, which is noncontiguous from any of the nearby residues (Figure 8A, red arrow). The electron density is close to the Cu atom but too distant to be assigned to a metal-coordinating water molecule. We thus assigned this density to a part of the free imidazole molecule accommodated in the cavity of H592A. In Figure 8A, the imidazole was temporarily modeled so that one of the two imidazole nitrogen atoms would become a ligand for the bound Cu (consequently, Cu is five-coordinate) and the other would be hydrogen-bonding to a water molecule (Wat1). However, this model may not be necessarily valid crystallographically, since the electron density was insufficient for structure modeling of the free imidazole molecule with a high occupancy or a low B factor or both. Nevertheless, comparison of the superimposed active-site structures (Figure 8C) shows that the free imidazole is placed nearly in the same position as the side-chain imidazole ring of His592 when it is in the major conformation (conformer *a*) in the WT-holo-AGAO structure (*14*); positional difference of the two imidazole rings is only about 1.8 Å when compared at the center of the rings. Presumably, the presence of the side-chain methyl group of Ala592 in H592A mutant would not allow the exact placement of the free imidazole in the position of the side-chain imidazole ring of His592 due to steric hindrance.

The Cu atom in H433A is coordinated with the $N^{\epsilon 2}$ atom of His431, the $N^{\delta 1}$ atom of His592, the phenolic oxygen atom of unmodified Tyr382, and an oxygen atom of a water molecule (Wat2) in a tetrahedral geometry (Figure 8B). This Cu-coordination structure is very similar to that observed in the initial intermediate formed during the TPQ biogenesis in AGAO crystals (*16*), except that a water molecule (Wat2) replaces the imidazole $N^{\epsilon 2}$ atom of the mutated His433. The distance between the Cu center and the phenolic oxygen atom of Tyr382 is 2.5 Å, which is within inner sphere coordination to the metal but not close enough to allow LMCT that is generally formed at a distance below 2.0 Å (*31, 32*). Besides the active-site Cu, binding of a second Cu was also identified in H433A mutant to the residues located on the molecular surface (Asp165, His170, and His201). However, the second Cu-binding may be fortuitously derived from the use of a high concentration (2 mM) of $CuSO_4$ for crystal soaking, because this site is different from those reported previously for ECAO (*11*), PSAO (*13*) and AGAO (*14*).

DISCUSSION

We have shown here that the TPQ-generating activity of H592A mutant of AGAO is rescued by exogenous imidazole. The rescue is likely through assistance of the binding of Cu^{2+} ion that is essential for generation of TPQ (*7*). The X-ray crystal structure of the imidazole-rescued holo-H592A mutant has suggested that an imidazole molecule is indeed bound within the cavity of H592A (Figure 8C) and surrogates for the missing side chain of His592. Such chemical rescue of mutant enzymes by exogenous compounds that complement the side chain of the mutated residue was demonstrated earlier for the active-site mutants of aspartate aminotransferase (*35*) and leucine dehydrogenase (*36*), where activities of the totally inactive lysine-to-alanine mutants were partially restored by addition of primary amines with various pK_a values, acting as a catalytic base. Subsequently, chemical rescues using imidazole and pyridine derivatives have also been reported for the mutants of several heme proteins containing a histidine residue as a proximal iron ligand, horseradish peroxidase (*37*), soluble guanylate cyclase (*38*), and sperm whale myoglobin (*39*). In those studies, replacement of a bulky functional residue, such as lysine and histidine, by a nonfunctional small one, such as glycine and alanine, was expected to create a cavity in the protein active site, allowing various compounds to be accommodated within the cavity and to restore the missing functionality.

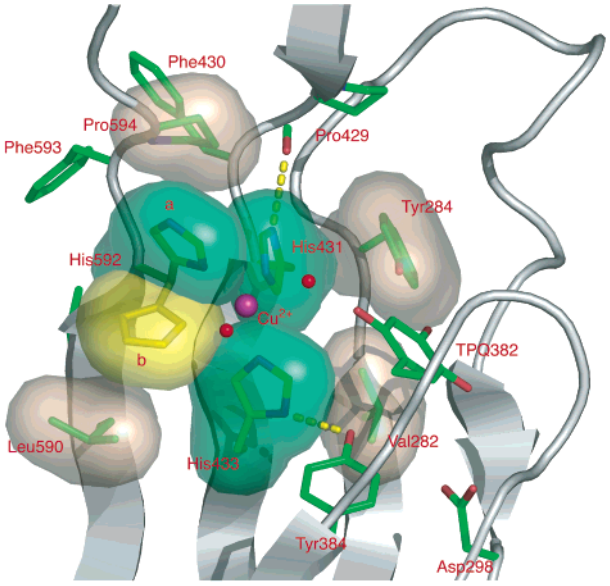

FIGURE 9: Interactions of Cu^{2+}-coordinating histidine residues with neighboring residues. The main and side chains of the active site residues of WT (1AV4) are shown in ribbon and stick models, respectively. The molecular surfaces of the side chains are also shown for Val282, Tyr284, His431, His433, Leu590, His592, and Pro594. The copper atom and its coordinating water molecules are shown by purple and red spheres, respectively. The major (*a*) and minor (*b*) conformers of His592 are colored differently. Hydrogen bonds to the side chain imidazoles of His433 and His431 are indicated by dotted yellow lines. This diagram was prepared using a PyMol molecular graphic system (DeLano Scientific, San Carlos, CA).

In the apo-AGAO structure determined previously (*14*), the vacant Cu-binding site is comprised with the imidazole nitrogen atoms of three histidine residues (His431-$N^{\epsilon 2}$, His433-$N^{\epsilon 2}$, and His592-$N^{\delta 1}$) and the 4-hydroxyl oxygen atom of Tyr382 (precursor to TPQ) arranged in an approximately tetrahedral geometry. In contrast, the TPQ ring in the holo-AGAO structure is tilted away from the Cu site, and the Cu atom is coordinated with the same three histidine residues and two additional water molecules in an approximately square-pyramidal geometry. Structural comparison of the two forms has also revealed that only His592 among the three Cu-binding histidine residues has dual conformations (conformers *a* and *b*), which differ by about 70° rotation around the $C^{\alpha}-C^{\beta}$ bond (*14*) (Figure 9). It appears that this conformational flexibility of His592 is allowed by the presence of a wide space beside its side chain imidazole, facing to a large water-filled cavity between the two subunits (*14*), through which an exogenous imidazole molecule may enter to the active site. By contrast, the side chain imidazole of His431 is positioned in a rather narrow space surrounded by residues Pro594, Tyr284, and His592 (conformer *a*) with its imidazole $N^{\delta 1}$ atom hydrogen-bonding to the main chain carbonyl O atom of Pro429 (Figure 9). The side chain imidazole of His433 is also buried in the protein interior and located close to the hydrophobic side chain of Val282 with its imidazole $N^{\delta 1}$ atom hydrogen-bonding to the phenolic O atom of Tyr384. The conformational flexibilities of His431 and His433 are thus limited as compared to that of His592. Furthermore, the presence of the side chain methyl group in H431A and H433A mutants, albeit much smaller than the imidazole group, would not allow an exogenous imidazole molecule to enter into the cavity without significant conformational changes of the surrounding residues. Collectively, these structural differences among the three Cu-binding histidine residues probably account for the chemical rescue observable only for the H592A mutant.

UV−visible and RR spectral features of H433A added with Cu^{2+} ions closely resemble those of a tyrosinate-to-copper charge-transfer complex reported for galactose oxidase (*31*, *32*) and synthetic model compounds (*33*). It is possible that because of the absence of the imidazole side chain of His433, the Cu atom may be positioned slightly more closely to the phenolic oxygen atom of Tyr382 in H433A than in the WT-AGAO so that the LMCT complex can be formed. However, as estimated from the molar extinction coefficient of the tyrosinate-to-copper charge-transfer complex in galactose oxidase ($\epsilon = 9500\ M^{-1}\ cm^{-1}$ at 445 nm) (*34*), the LMCT complex may be formed in H433A mutant only as a minor and transient species. The crystal structure of Cu-soaked H433A also shows that the distance between Cu and the phenolic oxygen atom of Tyr382 is not close enough to form an LMCT complex. Furthermore, the species such as an LMCT complex has never been detected spectrophotometrically with the WT-AGAO (*7*, *29*), unlike HPAO, in which the tyrosinate-to-copper LMCT complex absorbing at 350 nm is formed during the cofactor biogenesis (*40*, *41*). These observations suggest that in the initial stage of TPQ biogenesis in AGAO (*16*) the full charge-transfer from the tyrosinate to Cu(II) may not be needed, but only a partial charge-transfer is sufficient for activating the phenol ring of Tyr382 to be attacked by molecular oxygen.

It is rather surprising that the imidazole-rescued H592A mutant possesses very low catalytic activity, even though TPQ has been formed significantly. The "Cu-on" conformation of the TPQ ring observed in the crystal structure of H592A is presumably not a reason for the low catalytic activity, because the decreased activity is mainly ascribed to the latter oxidative half-reaction on the basis of the observation that both substrate and inhibitor react with TPQ of H592A. We have recently proposed that the bound Cu participates in the oxidative half-reaction by providing a binding site for $1e^{-}$- and $2e^{-}$-reduced dioxygen species to be efficiently protonated and released (*19*). Presumably, the Cu-coordination structure of H592A with a free imidazole as one of the Cu-ligands is not suitable for the bound Cu to play such a role. In other words, the metal coordination structure in AGAO must be more strictly optimized for the catalytic reaction than for the cofactor biogenesis. In conclusion, the present study demonstrates that the three Cu-binding histidine residues are important for both TPQ biogenesis and catalytic activity. They provide stable binding of the essential metal ion and fine-tune its position in the center of the versatile coordination structure during the cofactor biogenesis and catalysis.

NOTE ADDED AFTER PRINT PUBLICATION

Minae Mure was inadvertently omitted as an author in the version published on the Web 02/05/04 (ASAP) and in the March 2, 2004, issue (Vol. 43, No. 8, pp 2178−2187). The correct electronic version was published 04/23/04, and a

Correction appears in the May 25, 2004, issue (Vol. 43, No. 20).

ACKNOWLEDGMENT

We thank Dr. M. Kim and Ms. M. Yoshimura, School of Science and Technology, Kwansei Gakuin University, for their help with X-ray data collection and processing. We also thank Dr. S. Kishishita for his help in enzyme purification.

REFERENCES

1. Janes, S. M., Mu, D., Wemmer, D., Smith, A. J., Kaur, S., Maltby, D., Burlingame, A. L., and Klinman, J. P. (1990) A new redox cofactor in eukaryotic enzymes: 6-hydroxydopa at the active site of bovine serum amine oxidase, *Science 248*, 981−987.
2. McIntire, W. S., and Hartmann, C. (1993) Copper-containing amine oxidases, in *Principles and Applications of Quinoproteins* (Davidson, V. L., Ed.) pp 97−171, Marcel Dekker, New York.
3. Knowles, P. F., and Dooley, D. M. (1994) Amine oxidases, in *Metal Ions in Biological Systems* (Sigel, H., and Sigel, A., Eds.) Vol. 30, pp 361−403, Marcel Dekker, New York.
4. Mu, D., Janes, S. M., Smith, A. J., Brown, D. E., Dooley, D. M., and Klinman, J. P. (1992) Tyrosine codon corresponds to topa quinone at the active site of copper amine oxidases, *J. Biol. Chem. 267*, 7979−7982.
5. Klinman, J. P., and Mu, D. (1994) Quinoenzymes in biology, *Annu. Rev. Biochem. 63*, 299−344.
6. Tipping, A. J., and McPherson, M. J. (1995) Cloning and molecular analysis of the pea seedling copper amine oxidase, *J. Biol. Chem. 270*, 16939−16946.
7. Matsuzaki, R., Fukui, T., Sato, H., Ozaki, Y., and Tanizawa, K. (1994) Generation of the topa quinone cofactor in bacterial monoamine oxidase by cupric ion-dependent autoxidation of a specific tyrosyl residue, *FEBS Lett. 351*, 360−364.
8. Cai, D., and Klinman, J. P. (1994) Copper amine oxidase: heterologous expression, purification, and characterization of an active enzyme in *Saccharomyces cerevisiae*, *Biochemistry 33*, 7647−7653.
9. Cai, D., and Klinman, J. P. (1994) Evidence of a self-catalytic mechanism of 2,4,5-trihydroxyphenylalanine quinone biogenesis in yeast copper amine oxidase, *J. Biol. Chem. 269*, 32039−32042.
10. Choi, Y.-H., Matsuzaki, R., Fukui, T., Shimizu, E., Yorifuji, T., Sato, H., Ozaki, Y., and Tanizawa, K. (1995) Copper/topa quinone-containing histamine oxidase from *Arthrobacter globiformis*. Molecular cloning and sequencing, overproduction of precursor enzyme, and generation of topa quinone cofactor, *J. Biol. Chem. 270*, 4712−4720.
11. Parsons, M. R., Convery, M. A., Wilmot, C. M., Yadav, K. D., Blakeley, V., Corner, A. S., Phillips, S. E., McPherson, M. J., and Knowles, P. F. (1995) Crystal structure of a quinoenzyme: copper amine oxidase of *Escherichia coli* at 2 Å resolution, *Structure 3*, 1171−1184.
12. Wilmot, C. M., Murray, J. M., Alton, G., Parsons, M. R., Convery, M. A., Blakeley, V., Corner, A. S., Palcic, M. M., Knowles, P. F., McPherson, M. J., and Phillips, S. E. (1997) Catalytic mechanism of the quinoenzyme amine oxidase from *Escherichia coli*: exploring the reductive half-reaction, *Biochemistry 36*, 1608−1620.
13. Kumar, V., Dooley, D. M., Freeman, H. C., Guss, J. M., Harvey, I., McGuirl, M. A., Wilce, M. C. J., and Zubak, V. M. (1996) Crystal structure of a eukaryotic (pea seedling) copper-containing amine oxidase at 2.2 Å resolution, *Structure 4*, 943−955.
14. Wilce, M. C. J., Dooley, D. M., Freeman, H. C., Guss, J. M., Matsunami, H., McIntire, W. S., Tanizawa, K., and Yamaguchi, H. (1997) Crystal structures of the copper-containing amine oxidase from *Arthrobacter globiformis* in the holo and apo forms: Implications for the biogenesis of topaquinone, *Biochemistry 36*, 16116−16133.
15. Li, R., Klinman, J. P., and Mathews, F. S. (1998) Copper amine oxidase from *Hansenula polymorpha*: the crystal structure determined at 2.4 Å resolution reveals the active conformation, *Structure 6*, 293−307.
16. Kim, M., Okajima, T., Kishishita, S., Yoshimura, M., Kawamori, A., Tanizawa, K., and Yamaguchi, H. (2002) X-ray snapshots of quinone cofactor biogenesis in bacterial copper amine oxidase, *Nat. Struct. Biol. 9*, 591−596.
17. Ho, S. N., Hunt, H. D., Horton, R. M., Pullen, J. K., and Pease, L. R. (1989) Site-directed mutagenesis by overlap extension using the polymerase chain reaction, *Gene 77*, 51−59.
18. Tanizawa, K., Matsuzaki, R., Shimizu, E., Yorifuji, T., and Fukui, T. (1994) Cloning and sequencing of phenylethylamine oxidase from *Arthrobacter globiformis* and implication of Tyr-382 as the precursor to its covalently bound quinone cofactor, *Biochem. Biophys. Res. Commun. 199*, 1096−1102.
19. Kishishita, S., Okajima, T., Kim, M., Yamaguchi, H., Hirota, S., Suzuki, S.,Kuroda, S., Tanizawa, K., and Mure, M. (2003) Role of copper ion in bacterial copper amine oxidase: spectroscopic and crystallographic studies of metal-substituted enzymes, *J. Am. Chem. Soc. 125*, 1041−1055.
20. Otwinowski, Z., and Minor, W. (1997) Processing of X-ray diffraction data collected in oscillation mode, *Methods Enzymol. 276*, 307−326.
21. Leslie, A. G. W. (1992) *Joint CCP4 and EESF-EACMB newsletter on protein crystallography*, SERC Daresbury Laboratory, Warrington, U.K.
22. Collaborative Computational Project Number 4 (1994) The CCP 4 suite: programs for protein crystallography, *Acta Crystallogr. D50*, 760−763.
23. Brünger, A. T. (1992) *X-PLOR, Version 3.1. A System for Crystallography and NMR*, Yale University Press, New Haven, CT.
24. De Biase, D., Agostinelli, E., De Matteis, G., Mondovi, B., and Morpurgo, L. (1996) Half-of-the-sites reactivity of bovine serum amine oxidase. Reactivity and chemical identity of the second site, *Eur. J. Biochem. 237*, 93−99.
25. Ruggiero, C. E., and Dooley, D. M. (1999) Stoichiometry of the topa quinone biogenesis reaction in copper amine oxidases, *Biochemistry 38*, 2892−2898.
26. Nakamura, N., Moënne-Loccoz, P., Tanizawa, K., Mure, M., Suzuki, S., Klinman, J. P., and Sanders-Loehr, J. (1997) Topaquinone-dependent amine oxidases: identification of reaction intermediates by Raman spectroscopy, *Biochemistry 36*, 11479−11486.
27. Nakamura, N., Matsuzaki, R., Choi, Y. H., Tanizawa, K., and Sanders-Loehr, J. (1996) Biosynthesis of topa quinone cofactor in bacterial amine oxidases. Solvent origin of C-2 oxygen determined by Raman spectroscopy, *J. Biol. Chem. 271*, 4718−4724.
28. Paz, M. A., Flückiger, R., Boak, A., Kagan, H. M. and Gallop, P. M. (1991) Specific detection of quinoproteins by redox-cycling staining, *J. Biol. Chem. 266*, 689−692.
29. Matsuzaki, R., Suzuki, S., Yamaguchi, K., Fukui, T., and Tanizawa, K. (1995) Spectroscopic studies on the mechanism of the topa quinone generation in bacterial monoamine oxidase, *Biochemistry 34*, 4524−4530.
30. Hirota, S., Iwamoto, T., Kishishita, S., Okajima, T., Yamauchi, O., and Tanizawa, K. (2001) Spectroscopic observation of intermediates formed during the oxidative half-reaction of copper/topa quinone-containing phenylethylamine oxidase, *Biochemistry 40*, 15789−15796.
31. Whittaker, M. M., DeVito, V. L., Asher, S. A., and Whittaker, J. W. (1989) Resonance Raman evidence for tyrosine involvement in the radical site of galactose oxidase, *J. Biol. Chem. 264*, 7104−7106.
32. Ito, N., Phillips, S. E. V., Stevens, C., Ogel, Z. B., McPherson, M. J., Keen, J. N., Yadav, K. D. S., and Knowles, P. F. (1991) Novel thioether bond revealed by a 1.7 Å crystal structure of galactose oxidase, *Nature 350*, 87−90.
33. Halfen, J. A., Jazdzewski, B. A., Mahapatra, S., Berreau, L. M., Wilkinson, E. C., Que, L., Jr., and Tolman, W. B. (1997) Synthetic models of the inactive copper(II)-tyrosinate and active copper-(II)-tyrosyl radical forms of galactose and glyoxal oxidases, *J. Am. Chem. Soc. 119*, 8217−8227.
34. Whittaker, M. M., and Whittaker, J. W. (2003) Cu(I)-dependent biogenesis of the galactose oxidase redox cofactor, *J. Biol. Chem. 278*, 22090−22101.
35. Toney, M. D., and Kirsch, J. F. (1989) Direct Brønsted analysis of the restoration of activity to a mutant enzyme by exogenous amines, *Science 243*, 1485−1488.
36. Sekimoto, T., Matsuyama, T., Fukui, T., and Tanizawa, K. (1993) Evidence for lysine 80 as general base catalyst of leucine dehydrogenase, *J. Biol. Chem. 268*, 27039−27045.
37. Newmyer, S. L., Sun, J., Loehr, T. M., and Ortiz de Montellano, P. R. (1996) Rescue of the horseradish peroxidase His-170 Ala

mutant activity by imidazole: importance of proximal ligand tethering, *Biochemistry 35*, 12788−12795.
38. Zhao, Y., Schelvis, J. P. M., Babcock, G. T., and Marletta, M. A. (1998) Identification of histidine 105 in the β1 subunit of soluble guanylate cyclase as the heme proximal ligand, *Biochemistry 37*, 4502−4509.
39. Decatur, S. M., Belcher, K. L., Rickert, P. K., Franzen, S., and Boxer, S. G. (1999) Hydrogen bonding modulates binding of exogenous ligands in a myoglobin proximal cavity mutant, *Biochemistry 38*, 11086−11092.
40. Dove, J. E., Schwartz, B., Williams, N. K., and Klinman, J. P. (2000) Investigation of spectroscopic intermediates during copper-binding and TPQ formation in wild-type and active-site mutants of a copper-containing amine oxidase from yeast, *Biochemistry 39*, 3690−3698.
41. Schwartz, B., Dove, J. E., and Klinman, J. P. (2000) Kinetic analysis of oxygen utilization during cofactor biogenesis in a copper-containing amine oxidase from yeast, *Biochemistry 39*, 3699−3707.
42. Esnouf, R. M. (1997) An extensively modified version of MolScript that includes greatly enhanced coloring capabilities, *J. Mol. Graph. Modell. 15*, 132−134.
43. Merritt, E. A., and Bacon, D. J. (1997) Raster3D: Photorealistic molecular graphics, *Methods Enzymol. 277*, 505−524.

BI0361923